Biophysical Journal, Volume *116*

Supplemental Information

Nanobody-CD16 Catch Bond Reveals NK Cell Mechanosensitivity

Cristina González, Patrick Chames, Brigitte Kerfelec, Daniel Baty, Philippe Robert, and Laurent Limozin

SUPPLEMENTARY MATERIAL

Nanobody-CD16 catch bond reveals NK cell mechanosensitivity

Cristina Gonzalez, Patrick Chames, Brigitte Kerfelec, Daniel Baty, Philippe Robert, Laurent Limozin

Supplementary Methods

Surfaces preparation for molecular measurements with the laminar flow chamber

For laminar flow chamber (LFC) experiments, glass slides of 75x25 mm^2 (VWR) were rinsed twice with ethanol 98% and distilled water, then deposited 10 min in a solution containing 2/3 H_2SO_4 at 93-98 % and 1/3 of H_2O_2 at 50 % (both Sigma-Aldrich) then rinsed thoroughly with deionized water. Negative charged glass slides were incubated 10 min with a solution of 100 μg/ml of polylysine (Poly-L-lysine hydrobromide 150000-300000 kDa, Sigma-Aldrich) in phosphate buffer 0.01 M pH= 7.4 with 0.01% azide. Slides were subsequently washed with PBS and incubated 10 min with 25 mg/ml of glutaraldehyde in borate buffer (H_3BO_3 + H_2O) 0.1M pH=9 with 0.01 % azide. Amine groups of polylysine make covalent bonds with one of the aldehyde groups of glutaraldehyde. After washing with PBS, another incubation of 10 min with 100 μg/ml of BSA biotin (Sigma-Aldrich) in PBS was performed. Glass slides were washed with PBS and incubated for 10 min with a solution of 0.2 M glycine in PBS + 0.1% BSA for neutralization of remaining free aldehyde groups. After washing with PBS, slides were incubated for 30 min with 10 μg/ml of a solution of streptavidin (Sigma-Aldrich) in PBS. Finally, after washing with PBS, slides were deposited on the bottom of the LFC and 100 μl of biotinylated nanobodies were incubated for 30 min at various concentration in each compartment, before a final rinsing with PBS.

Measurement of surface density of antibodies

Samples were imaged using a microscope Observer (Carl Zeiss) equiped with an objective 20x/0.8, a 200 W light source (Lumen200, Prior) set at 10% power and an additional neutral filter (transmission 30%) to reduce photobleaching. Illumination aperture was set to 0.95. Fluorescence was excited and collected with the following filterset: EX 546/12 nm - BS 560 nm - EM 575-640 nm. Images were recorded, using an Andor iXon camera and Micro Manager software, at different exposure times (50, 100, 200, 500 ms) depending on the fluorescence intensity of the sample, in order to optimize the signal. 10-20 fields were imaged for each sample. For the analysis, a region of interest (ROI) was defined for all images using Image J giving mean intensity values and the standard deviation for all the ROI of each image (Fig. S1C). From this mean value, the intensity given by the offset of the camera was removed and the result was divided by the exposure time. To retrieve the surface density of fluorescent molecules from the intensity, a calibration was performed by measuring the fluorescence of a known amount of fluorescent antibody in a 10 μm thin volume (22) (Fig. S1D). The relation between surface density of antibody and incubation concentration was finally determined (Fig. S1E).

Antibody binding at cell surface by flow cytometry

Nanobody specific binding to CD16 at cell membrane was measured by flow cytometry. Briefly, the nanobodies attached to CD16 on NK cell surface were detected using a secondary fluorescent antibody (anti HIS-PE, Milteny Biotec) which binds to the His tag of the nanobody. 200.000 NK cells were centrifuged at 400 g during 3 min and resuspended in the appropriate volume of a solution of PBS-BSA 1%. Then, 200 μl of the suspension containing NK cells were deposited into wells of a 96 well plate with U bottom. Well plates were centrifuged at 400 g during 3 min and incubated in a solution of 100 μl of PBS-BSA 1% with the biotinylated nanobodies at different concentrations during 45 min at 4°C. Then cells were rinsed with a total of 300 μl of PBS-BSA 1% and incubated in a solution of 100 μl of antiHIS-PE (1/20) during 1h at 4°C. Finally, cells were rinsed with 300μl of PBS-BSA 1% and re-suspended in 200 μl of PBS-BSA 1% before the measurement, which was performed using a flow cytometer (MACSQuant, Miltenyi Biotec). In the case of primary NK cells, their purity was check after isolation from red blood cells using additional staining was made using anti-CD3 FITC antibody (Miltenyi Biotec, dilution 1/50) and anti-CD56 APC (Miltenyi Biotec, dilution 1/20); See Fig. S6. Positive control was performed using the conventional monoclonal antiCD16-PE (clone 3G8 Biolegend) at concentration 13 nM; negative control isotype: IGG2b-PE (Biolegend).

Surface and cell preparation for spreading experiments

Uncoated μ-Slide 8 wells were functionalized with single domain antibodies as follows: 100 μg/ml BSA biotin (Sigma Aldrich) was deposited directly on the device and incubated 30 min. Then, devices were rinsed with PBS and incubated 30 min with 10 μg/ml streptavidin (Sigma Aldrich) in PBS. Biotinylated nanobodies C21 or C28 were incubated at various concentrations during 30 min and devices were finally rinsed with PBS before cell deposition. A positive control was performed by replacing the

nanobody by a conventional anti-CD16 biotinylated mAb (clone 3G8, Biolegend). nanobodies density on surface was measured by fluorescence as described above. Before each experiment, 20.000 cells were collected from culture flasks, centrifuged 5 min at 1500 rpm, re-suspended in 200 μl of PBS-BSA 0.2 % and kept 10 min in Eppendorf tubes at 37 °C, before deposition in the device which was previously heated at 37 °C.

Image analysis procedure to determine spread and non-spread cells

Using Fiji distribution of ImageJ, Reflection (RICM) images were normalized by the background (to obtain reflectivity) and segmented as described previously (32). Briefly, a variance filter with a radius of 8 pixels or 1.6 μm was applied to the reflectivity image, followed by a threshold at comprised between 0.002 and 0.008. The Analyse Particle plugin of ImageJ was then applied to define Regions of Interest (ROI) with a minimal area (fixed to 1000 pixel or 40μm^2, in order to remove small defects on images) and a minimal circularity fixed to 0.1. Two examples of normalized RICM images and ROI are shown on Fig. S9B and D. The same procedure was applied to segment cells from transmission images; the radius of variance was fixed to 5 pixel (or 1μm), the minimal area fixed to 2000 pixel or 80μm^2 (higher than RICM images as in this case we focus on cells selection, not in spread area) and the minimal circularity fixed to 0.3. Transmission images with the ROI are shown on Fig. S9A and C.

Coordinates, area, mean and standard deviation of the intensity of all the ROI in reflection and transmission were measured using Fiji and transfered to Igor Pro software (Wavemetrics). A second threshold of size was made in order to remove cells fragments. ROIs with an area below 3500 pixels (140 μm^2) in transmission were removed except if the spread area (RICM) was above 3000 pixels (120μm^2). Based on the reflectivity properties on the negative control (no spread cells) and on the positive control (almost all spread cells), ROI were divided into 4 populations (P1, P2, P3, P4) in order to distinguish spread and non-spread cells as shown in Fig. S10. P1 are ROI detected in reflection but not in transmission, corresponding to highly spread cells. P2 are ROI detected both in reflection and transmission with mean reflectivity below 1.07 and sd reflectivity below 0.06, corresponding to spread cells. P3 are ROI detected in transmission but not in transmission, with mean reflectivity values between 1.02 and 1.07 and sd reflectivity values below 0.06, corresponding to non spread cells. ROI corresponding to non-spread cells show as white patches in reflection and detected as ROI. To account for that, the population P4 was defined as ROI which appeared in transmission and reflection with the same reflectivity values as P3 (mean reflectivity values between 1.02 and 1.07 and standard deviation reflectivity values below 0.06) corresponding to non-spread cells. Once cells were classified into the 4 populations, spread cell fraction was calculated as $SF = \frac{P1+P2}{P1+P2+P3+P4}$.

Mean spread area and SEM from cells P1 and P2 (spread cells) were calculated. To quantify the tightness of cell surface-contact, mean and SEM reflectivity from cells P1 and P2 were calculated. For kinetics of spreading experiment, ROI were detected from reflection and their spread area was measured. In Igor Pro, knowing the position of the cells on the images, a criteria of minimal distance between the cells of different images was established and allowing individual cells to be tracked over all the stack of RICM images (32). Elapsed time between images was saved in metadata folder and used to track the spread area of cell over the time.

For the analysis of primary NK cell spread experiments, the same procedure was applied with adjustment of the following parameters to account for specificities of these cells: i) The minimal spread area for detection with ImageJ was fixed to 500 pixels or 20μm^2 to adapt to the smaller size of primary NK cells compared to NK92-CD16. The minimal size in transmission was set to 20μm^2. Contrary to NK92 culture, no cellular debris are found. In Igor Pro, size threshold were also set to 20μm^2. ii). The thresholds for reflectivity were adjusted to 1.01 and 1.1 and to 0.1 for the standard deviation of the reflectivity. iii) Finally, red blood cells were removed from P1 and P2 population; they correspond to a reflectivity above 1 and 1.03 respectively, simultaneously with the area in reflection lower than 88 μm^2.

Supplementary Figures

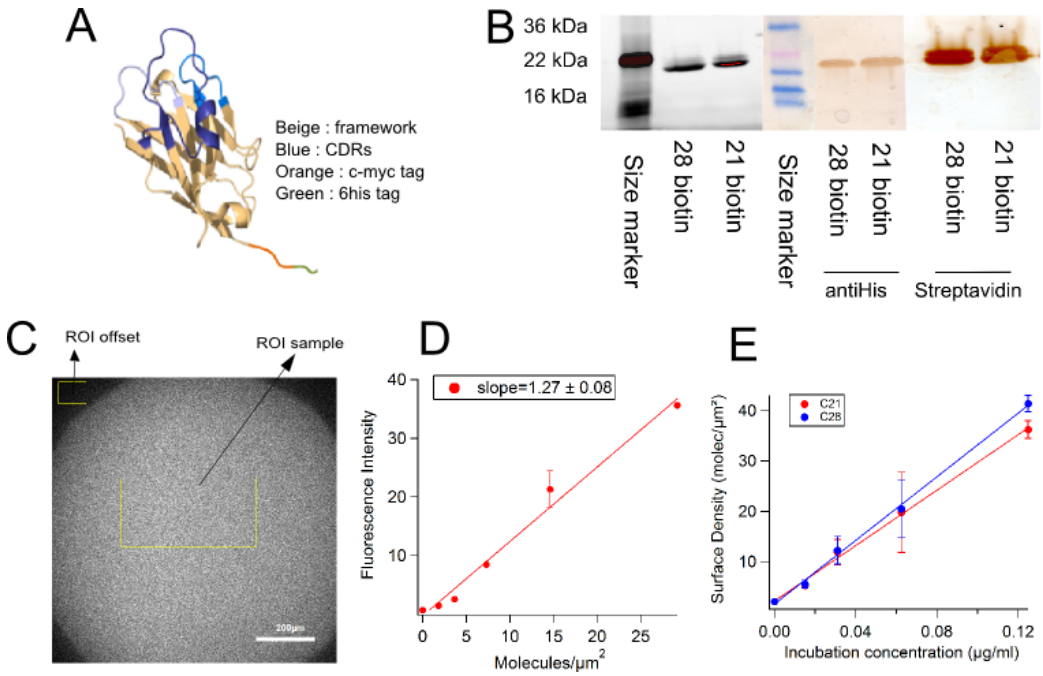

Figure S1: Nanobody structure, biotinylation process and use for surface functionalisation. A. Schematic representation of the nanobodies C21 or C28 with the corresponding His and c-Myc tag. B. Gel and Western Blot of C21 and C28 after biotinylation. On the gel, the strongest band corresponds to molecular weight of nanobodies (MW=15 kDa). On the Western Blot, anti His staining shows the presence of nanobodies C21 and C28 via the His tag and Streptavidin staining reveals the biotinylation of these nanobodies. C. Density of nanobodies on surfaces assessed using the detection of the Histag with a PE conjugated anti-His mAb. The image shows the fluorescence obtained after depositing 0.125 μg/ml of nanobody C28 on the slide. The yellow rectangle visualizes the selected ROI for intensity measurement. D) Calibration curve giving the fluorescence intensity of anti-His-PE fluorescence antibody as function of the number of molecules/μm^2. The slope of the linear fit b=1.27 was used to determine nanobodies density. E) Graph showing the molecular density as function of the concentration of incubation of nanobodies. The density factor is the slope of the concentration *vs* density line.

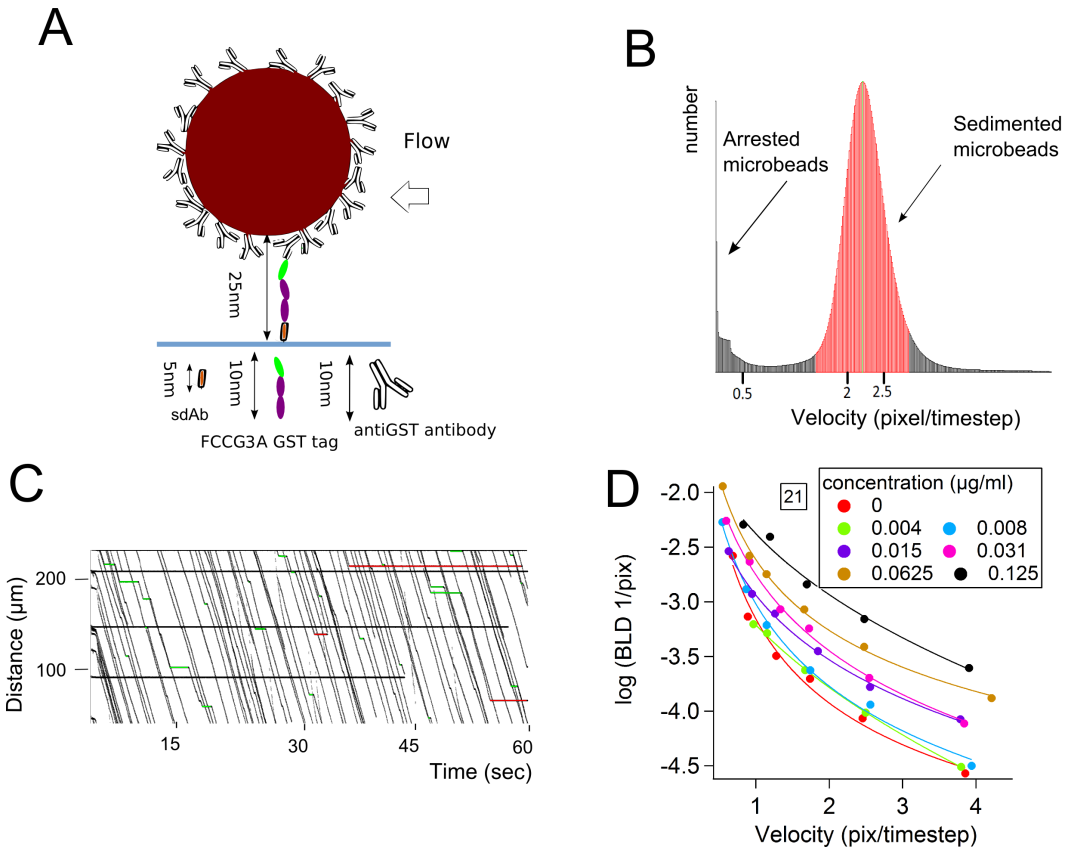

Figure S2: Laminar Flow Chamber for single bond kinetic measurements. A) Schematic representation of the strategy used to measure nanobodies-antigen interaction. FcγRIIIA (CD16) is coated to the microsphere via the anti-GST antibody and nanobodies are on the functionalised surface. Approximate length of all molecules is represented. Due to random orientation of the anti-GST antibody bound to the microsphere surface, an average length of 10 nm is considered. Total length of the molecular chain L=25 nm is represented and used to calculate, at a given shear rate, the molecular encounter time before bond formation and the force applied before bond rupture. B) Velocity histogram showing the peak of the arrested microspheres and the peak of the sedimented microspheres. C) Typical set of microsphere trajectories. Arrested microspheres are represented with a straight bar in green when the duration of the arrest is known and in red when is unknown. D) Interpolation of measured BLD as a function of microsphere velocity for each incubation concentration. Each data point corresponds typically to 4 independent experiments.

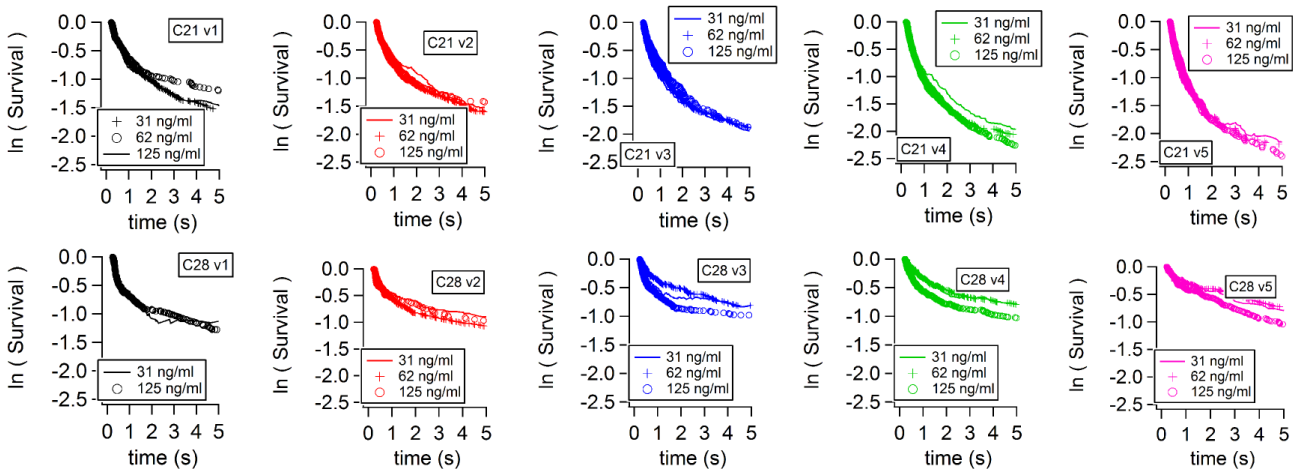

Figure S3: Superimposed survival curves for single bond assessment. Specific survival curves for nanobodies C21 (top row) and C28 (bottom row). Nanobodies were incubated at concentrations at 31, 62, 125 ng/ml and microsphere velocities were measured at 15, 21, 29, 41, 58 μm/s. Curves superimposition at various molecular density of nanobody show that the dissociation kinetics do not depend on density, strongly supporting the measurement of single antibody-antigen bonds.

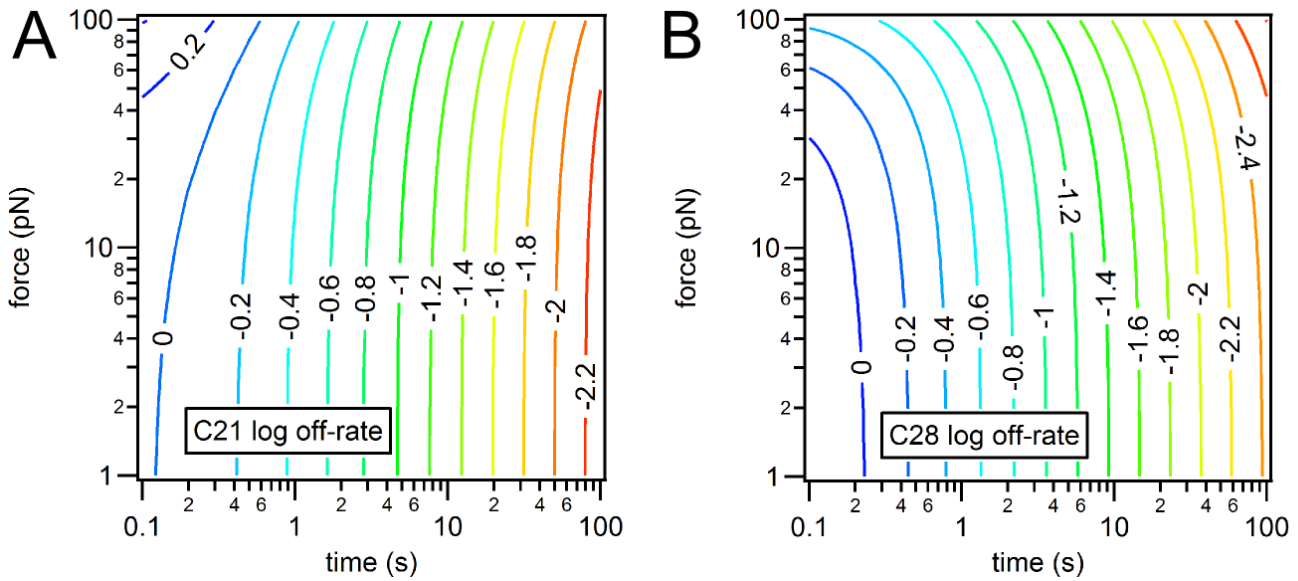

Figure S4: Logarithm of off-rates for C21 (A) and C28 (B) as function of applied force and lifetime of the bond. Values are calculated using Eq. 1 with measured parameters from Table 1.

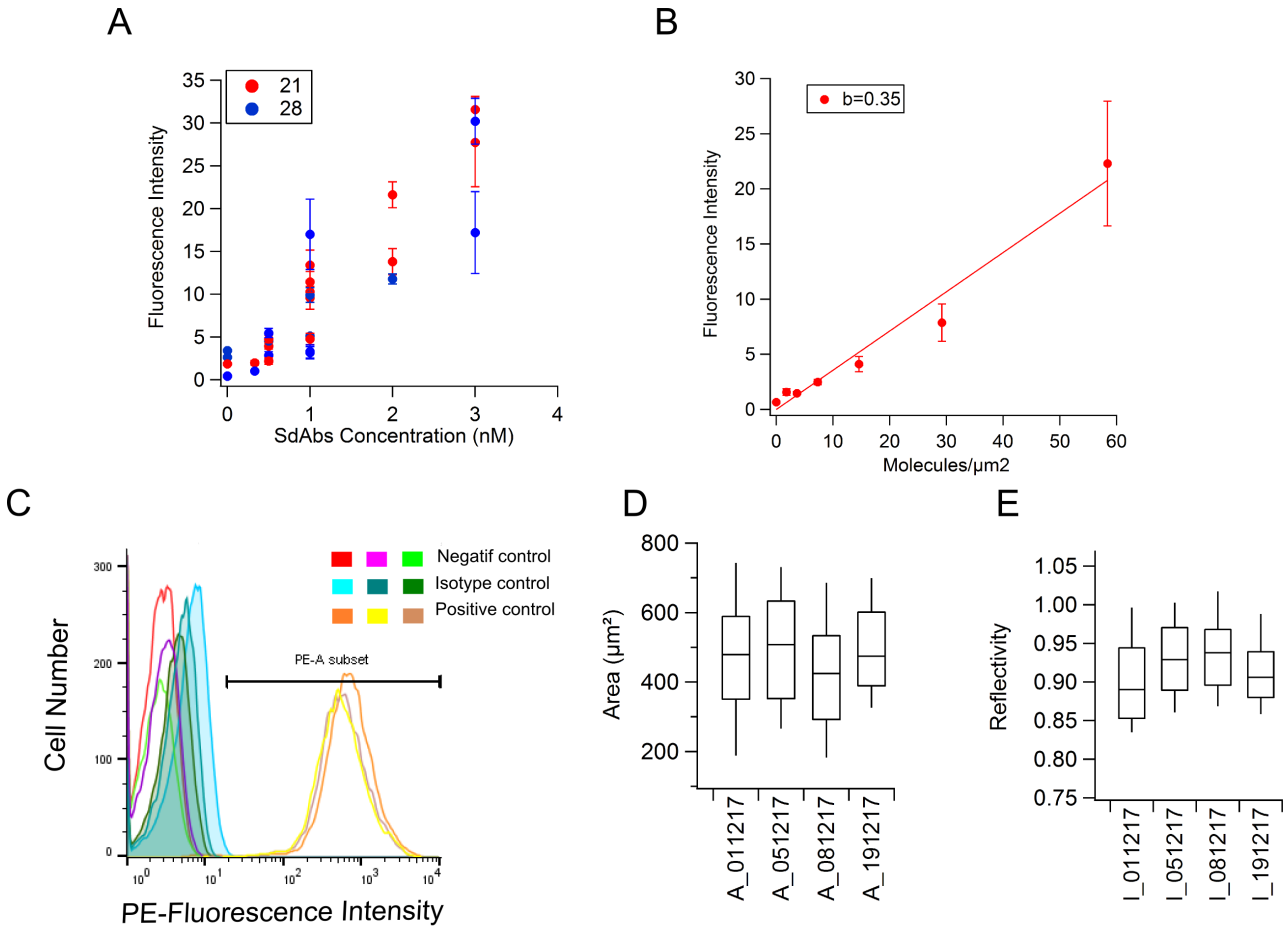

Figure S5: Controls of nanobody coated surfaces and NK92-CD16 cells. A) Fluorescence intensity values corresponding to the concentration of nanobody incubated on the Ibidi surface. (Fluorescence surface control was done at the end of the experiment). B) Calibration of the fluorescence intensity as a function of the surface density of nanobodies at the surface C) Fluorescence intensity histograms obtained by flow cytometry showing CD16 expression on NK cells. Superimposed positive curves indicate that CD16 expression is stable throughout all the period of cell culture. D,E) Distribution for four representative experiments of NK spreading area (D) and reflectivity (E) values obtained on surfaces coated with conventional anti-CD16 (clone 3G8), taken as a positive control for spreading. NK92-CD16 cell spreading with anti-CD16 coated surfaces was similar in all the experiments.

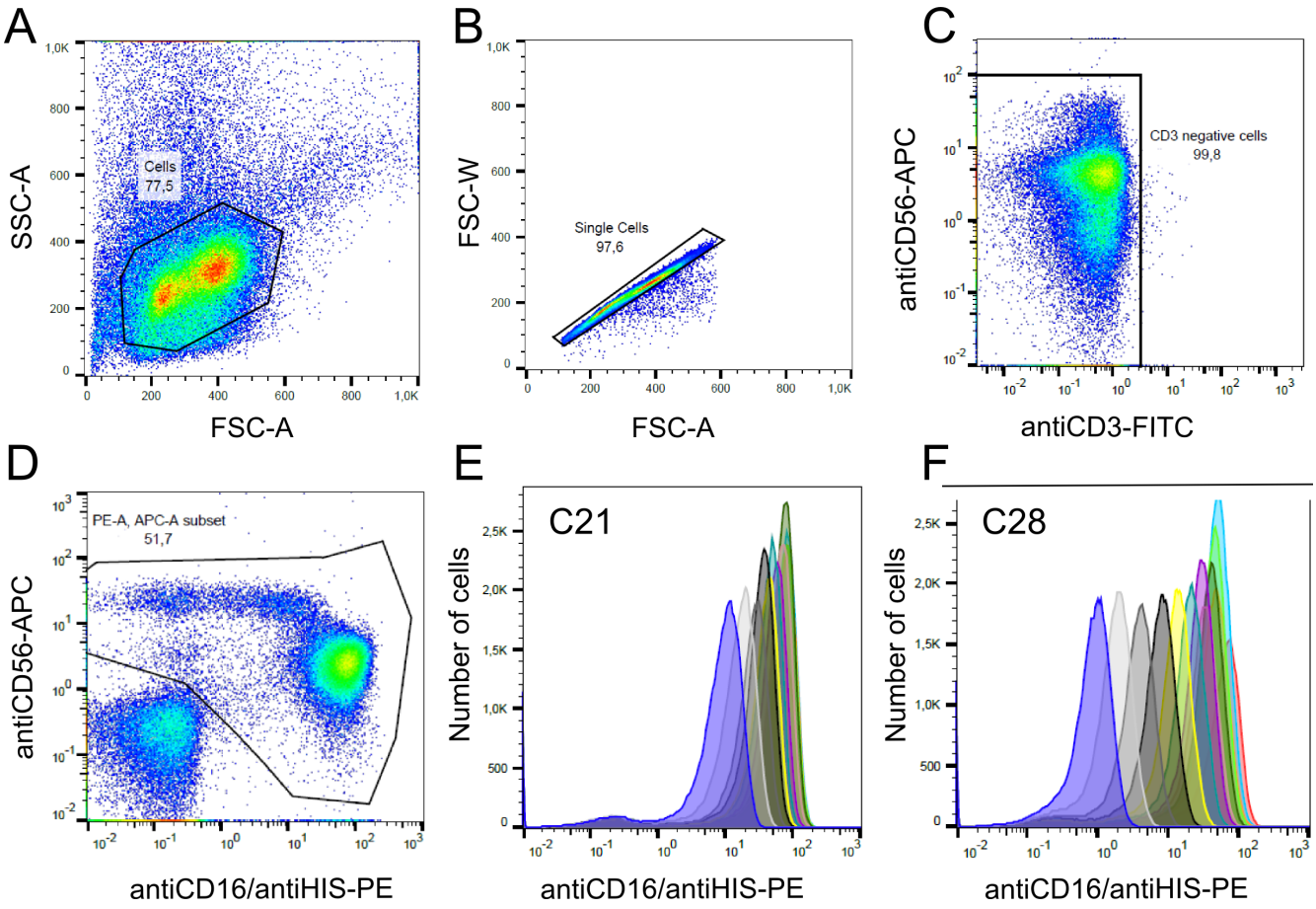

Figure S6: Gating procedure for the selection of purified primary NK cells by flow cytometry. A, B) Selection of cell population based on foward and side scatter signals. C) Selection of CD3 negative cells using an antibody anti-CD3 FITC highlighting the absence of CD3 positive cells like T lymphocytes. D) Selection of NK cell populations (CD56 bright and CD56 dim) using the antibody antiCD16-PE (positive control) and an antibody anti-CD56-APC. E, F) Histograms characterizing the selected NK cell populations representing the distribution of fluorescence intensity of the antiHIS-PE coupled to the biotinylated sdAbs C21 (E) and C28 (F) used at several dilutions.

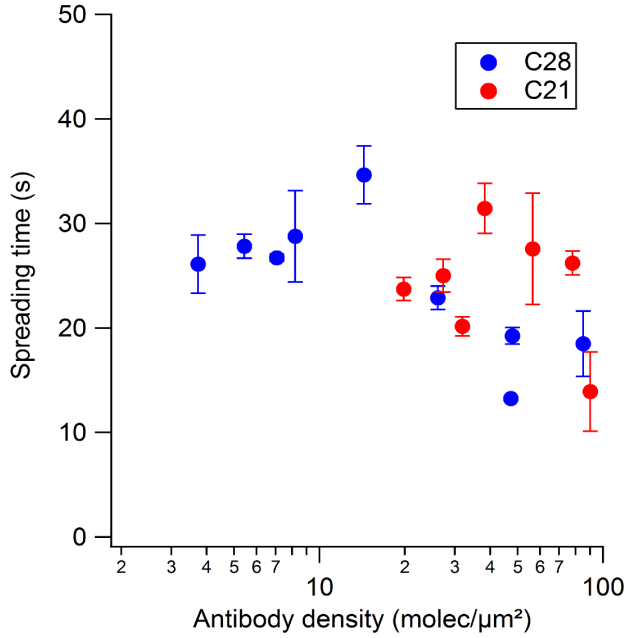

Figure S7: Cell Spreading kinetics. Individual NK92-CD16 cells engaging on surface coated with various densities of nanobodies were monitored over time with RICM. Spreading area versus time curves were fitted using a sigmoidal curve with time constant reported on the y axis. Each point and error bar represent the average and SEM of at least 10 cells.

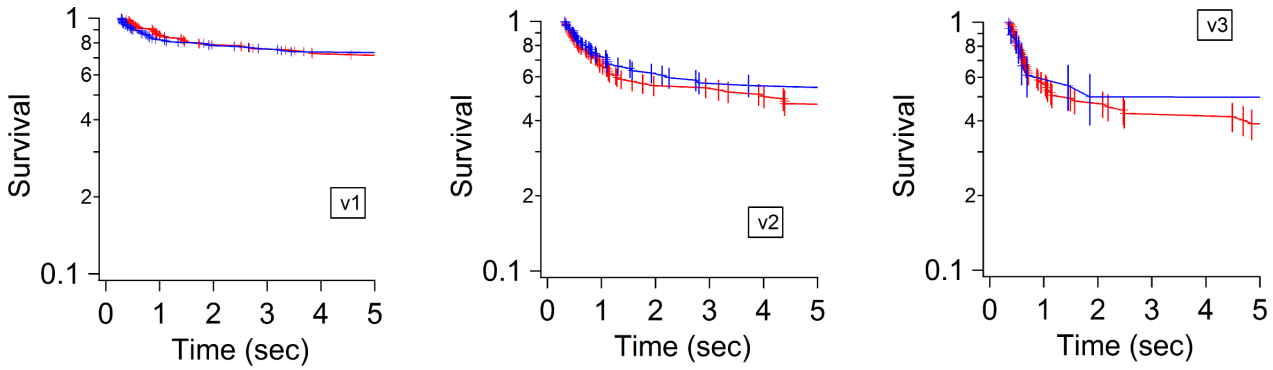

Figure S8: Survival curves of the transient adhesion of NK92-CD16 cells on nanobodies anti-CD16 coated surfaces (nanobodies density values on surface were between 6.5-12 molecules/μm^2) measured with the laminar flow chamber at shear stress of A) 0.075, B) 0.3 and C) 0.6 dyn/cm^2. Red: C21; Blue: C28. Survival curves are built by the pool of arrested cells from at least three independent experiments.

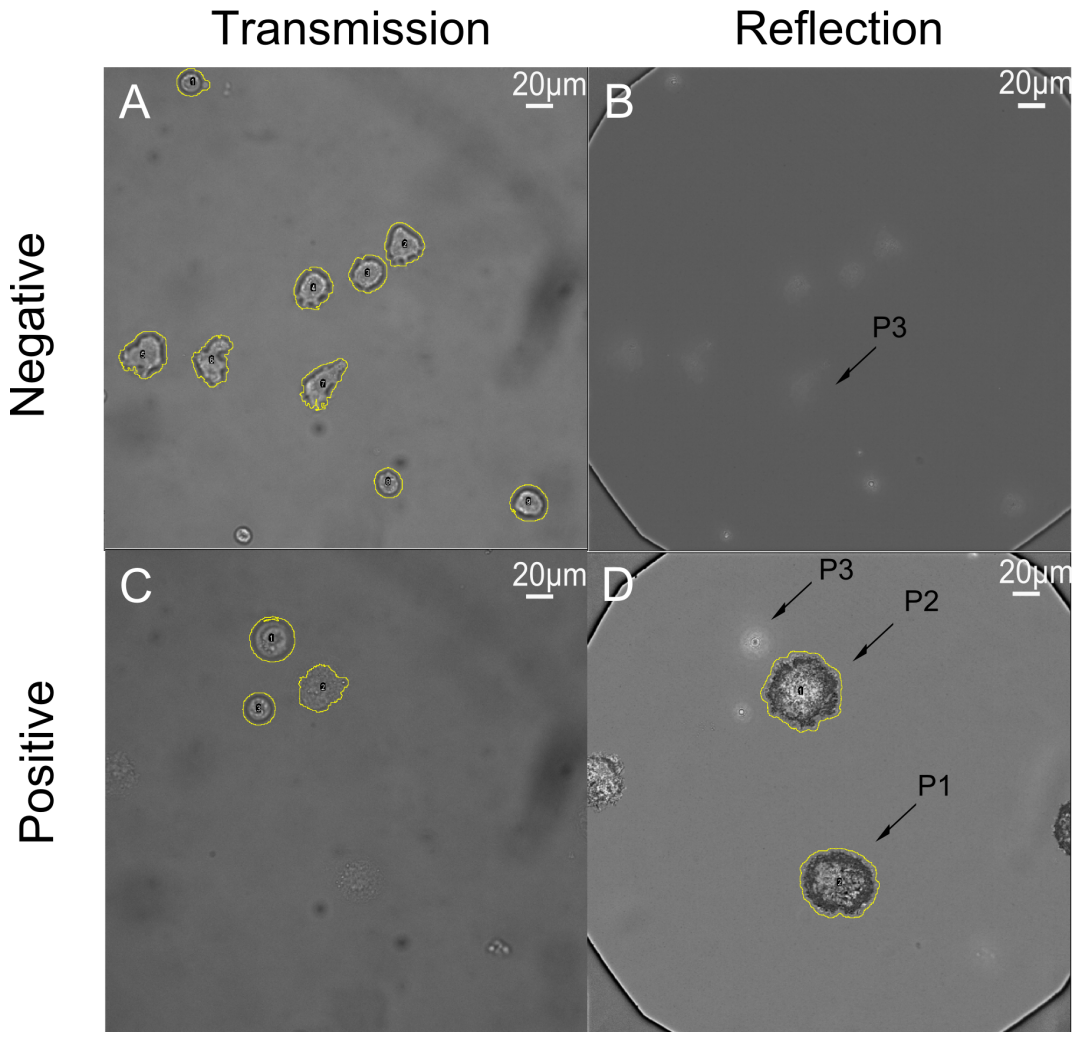

Figure S9: Images and procedure of segmentation of NK92-CD16 cells on anti-CD16 surfaces. A-B) Negative control (without nanobody on surface) showing the population P3 (no spread cells) as cells detected in transmission and not in reflection. C-D) Positive control, showing spread cells distributed among different subpopulations: P1 (detected only in RICM) and P2 (detected on both images) as well as non spread cells (P3).

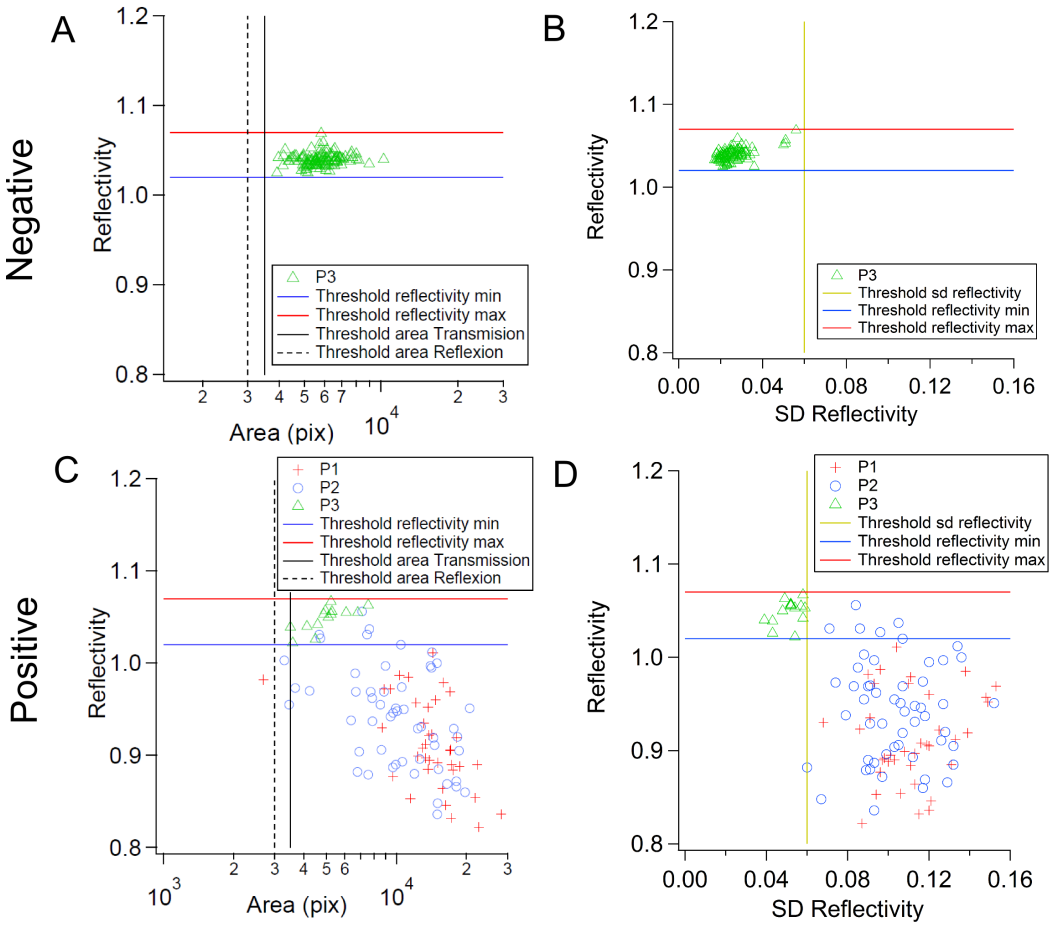

Figure S10: Graphs used to determine the parameters which defined the different populations of NK92-CD16 cells in microscopy. A. Graph of a negative control showing thresholds of area and mean reflectivity used for non-spread cells selection and P3 population between reflectivity thresholds. B. Graph of the same negative control showing the threshold of sd reflectivity and P3 population under the sd reflectivity threshold. C-D. Graphs of a positive control showing the thresholds of area, mean (C) and sd reflectivity (D) and the different spread populations (P1 and P2) separated from the non-spread population (P3).

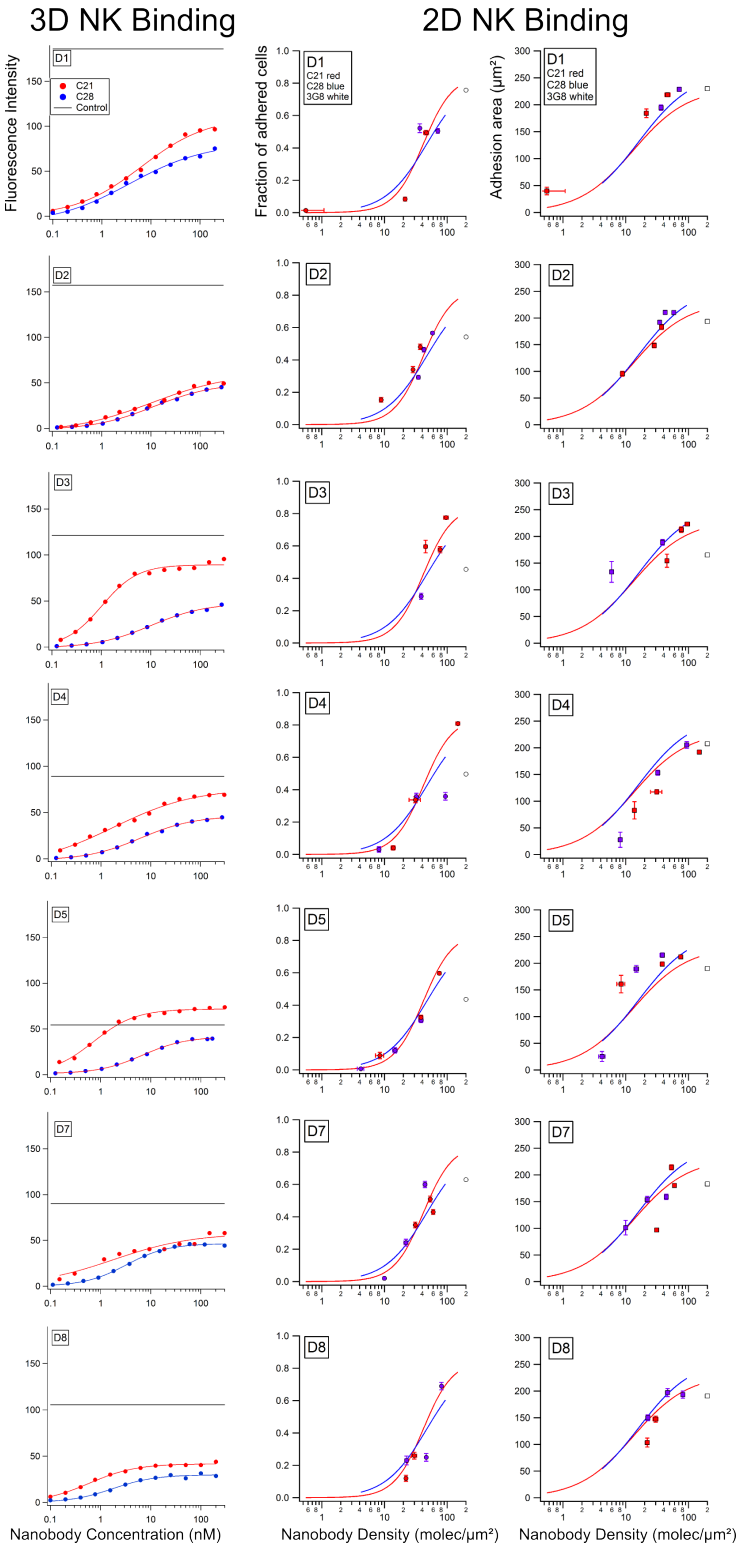

Figure S11: Comparison of 3D and 2D binding of anti-CD16 C21 and C28 nanobodies to NK primary cells obtained from 7 donors (raws D1-D5,D7,D8). Column 1: 3D binding of nanobodies on cell surface measured by flow cytometry: median fluorescence intensity vs nanobody concentration. The horizontal black line represents mfi obtained with a fluorescent anti-CD16 mAb (clone 3G8). Column 2-3: Spreading of NK cells on nanobody coated surfaces measured by RICM: Fraction of spread cells vs nanobody surface density (Column 2); spreading area of spread cells vs nanobody surface density (Column 3).

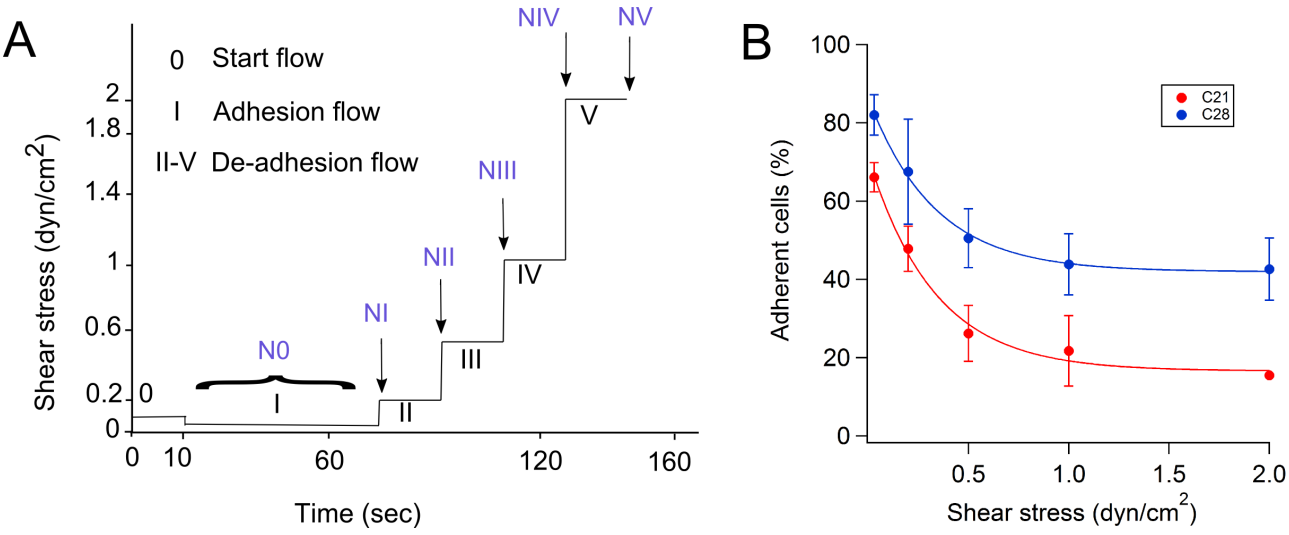

Figure S12: Detachment of NK92-CD16 cells adhering on nanobodies coated surfaces by a flow. A) Time sequence of the shear stress imposed on adhering NK cells in the laminar flow chamber. Most of the cells adhere to the surface during the period I (adhesion flow), and de-adhere during force steps II-V. B) Fraction of attached cells on nanobody coated surfaces at the various imposed shear stress. Nanobody coated densities were between 6.5 and 15 molecules/μm^2. Points represents mean values of 2 or 3 independent experiments. Number of total adherent cells detected were > to 50 for both nanobodies. Error bars are the standard deviations.